Structure of PS−PEO Diblock Copolymers in Solution and the Bulk State Probed Using Dynamic Light-Scattering and Small-Angle Neutron-Scattering and Dynamic Mechanical Measurements

Kell Mortensen,*,† Wyn Brown,‡ Kristoffer Almdal,† Elouafi Alami,‡ and Amane Jada§

Condensed Matter Physics and Chemistry Department, Risø National Laboratory, Roskilde, Denmark, Department of Physical Chemistry, Uppsala University, Sweden, and Centre de Recherches sur la Physico-Chimie des Surfaces Solides, Mulhouse, France

Received October 1, 1996. In Final Form: April 18, 1997⊗

The phase behavior of a low molecular weight ($M_W = 4000$) diblock copolymer of polystyrene and poly(ethylene oxide), PS−PEO, in the bulk as well in aqueous, D_2O, solutions has been studied using small-angle neutron-scattering, dynamic and static light-scattering, and rheological methods. At low temperature the pure block copolymer forms a lamellar mesophase driven by the crystallization of PEO. The melting point of PEO, $T \approx 64$ °C, is correspondingly accompanied by an order-to-disorder transition. The melt is typified by single-exponential depolarized correlation functions in the dynamic light-scattering spectra, observed in the temperature range 60 to 100 °C. Neutron scattering fails to show concentration fluctuations in the amorphous, disordered phase due to lack of contrast. In aqueous solutions up to roughly 20% polymer concentration, PS−PEO self-associates into spherical micelles with a core size of $R_c \approx 56$ Å and an interaction radius $R_{hs} \approx 115$ Å, corresponding to an aggregation number of 470. The hydrodynamic radius $R_h = 140$ Å obtained from dynamic light scattering is close to but somewhat larger than the interaction radius, as expected. Extended clusters, displaying a small but significant anisotropy, form at above $C =$ 10% and coexist with the single spherical micelles. These clusters may be due to association of spherical micelles or micelles of different form attributed to residual aggregates of PS moities.

1. Introduction

The dynamics of diblock copolymer melts and solutions have recently attracted extensive interest on account of the diversity of phase morphologies and the resulting phase transitions.

While many block copolymers undergo order−disorder transitions as a consequence of enthalpy-driven phase separation on the length scale of the polymer size,[1] ordering on the mesoscopic length scale may also occur when one of the blocks crystallizes. Block copolymers of poly(ethylene oxide) typically show such ordering phenomena.[2−6]

As for the relatively well-studied low molecular weight surfactants, self-association of block copolymers is observed on dissolution in a selective solvent which is a good solvent for one block but a poor or nonsolvent for the other. Such materials typically associate into micellar aggregates which may, for example, be spherical, rodlike, or disks depending on the molecular makeup and the location in the phase diagram. In aqueous systems, block copolymers with poly(ethylene oxide) as the water-soluble part have recently attracted great interest both for their applications and in basic research.[9−12]

The present paper describes small-angle neutron-scattering, light-scattering, and rheological studies which are used to elucidate the structural features of the bulk as well as D_2O solutions of a relatively low molecular weight diblock copolymer of polystyrene (PS) and poly(ethylene oxide) (PEO). On the basis of fluorescence-probing and light-scattering methods, Winnik and co-workers[13,14] have earlier presented investigations of aqueous solutions of PS−PEO diblock as well as PEO−PS−PEO symmetrical triblock structures, revealing micelle formation and giving some properties of the micelles in solution. The present study concerns a PS−PEO 1-3 diblock copolymer with molecular weight $M_W = 4000$, where the 1-3 index denotes the PS and PEO block sizes of 1000 and 3000, respectively. The measurements cover a broad range of temperature and encompass a wide span of concentration in the D_2O solutions. In the bulk, the PS−PEO 1-3 diblock copolymer at low temperature forms a lamellar phase induced by the PEO crystallization into extended lamellae. At $T = 64$ °C the material undergoes an order−disorder transition into a homogeneous phase. In D_2O solutions up to roughly 20% copolymer, the PS−PEO 1-3 diblock copolymers form spherical micelles with a dense core of the PS moiety.

† Risø National Laboratory.

‡ Uppsala University.

§ Centre de Recherches sur la Physico-Chimie des Surfaces Solides.

⊗ Abstract published in *Advance ACS Abstracts,* June 15, 1997.

(1) Bates, F. S.; Fredrickson, G. H. *Annu. Rev. Phys. Chem.* **1990**, *41*, 525.

(2) Viras, F.; Luo, Y.-Z.; Viras, K.; Mobbs, R. H.; King, T. A.; Booth, C. *Macromol. Chem.* **1988**, *189*, 459.

(3) Mortensen, K.; Brown, W.; Jørgensen, E. *Macromolecules* **1994**, *27*, 5654.

(4) Mortensen, K.; Brown, W.; Jørgensen, E. *Macromolecules* **1995**, *28*, 1458.

(5) Yang, Y.-W.; Tanodekaew, S.; Mai, S.-M.; Booth, C.; Ryan, A. J.; Bras, W.; Viras, K. *Macromolecules* **1995** *28*, 6029.

(6) Hillmyer, M.; Bates, F. S.; Almdal, K.; Mortensen, K.; Ryan, A. *Science* **1996**, *271*, 976.

(7) Takahashi, Y.; Tadokoro, H. *Macromolecules* **1973**, *6*, 881. Tadokoro, H. *Structure of Crystalline Polymers*; Wiley: New York, 1979.

(8) Ryan, A. J.; Fairclough, P. A.; Hamley, I. W.; Mai, S.-M.; Booth, C. *Macromolecules*, in press.

(9) Chu, B. *Langmuir* **1995**, *11*, 414.

(10) Almgren, M.; Brown, B.; Hvidt, S. *Colloid Polym. Sci.* **1995**, *273*, 2.

(11) Alexandridis, P.; Athanassiou, V.; Hatton, T. A. *Langmuir* **1995**, *11*, 2442.

(12) Mortensen, K. *J. Phys. Condens. Matter* **1996**, *8*, A103.

(13) Xu, R.; Winnik, M. A.; Hallett, F. R.; Riess, G.; Croucher, M. D. *Macromolecules* **1991**, *24*, 87.

(14) Wilhelm, M.; Zhao, C.-L.; Wang, Y.; Xu, R.; Winnik, M. A.; Mura, J.-L.; Riess, G.; Croucher, M. D. *Macromolecules* **1991**, *24*, 1033.

S0743-7463(96)00963-8 CCC: $14.00

2. Experimental Section

A. Materials. The diblock copolymer polystyrene−poly(ethylene oxide), PS−PEO 1-3 ($[CH_2CHC_6H_5]_m-H[OCH_2CH_2]_n$), has a molecular weight of 4000, 1000 for the PS component and 3000 for PEO (corresponding to the average degree of polymerization $m = 9.6$ and $n = 68.2$). The copolymer was supplied by Goldschmidt AG and was used without further purification.

The samples of bulk copolymers were gently pressed into pellets and measured during both the initial heating and cooling and the second heating. While there was a major hysteresis between the heating and cooling cycles, there was no difference between data of initial and later heating runs.

The aqueous solutions of diblock copolymer were made by mixing the copolymer with water at room temperature and heating to above 60 °C to form the thermodynamically stable micelles. Deuterium oxide, D_2O, which was used for both the neutron- and light-scattering experiments, was used in order to get good contrast and low background in the neutron scattering experiments. Prior to annealing, the dilute solutions formed an opaque dispersion. The solutions discussed below are all given in weight percent (wt %).

The critical micellation concentration, cmc, was obtained by surface tension measurements and also by using a fluorescence method with pyrene as probe.

B. Rheology. Dynamical mechanical measurements were conducted using a Rheometrics RMS-800 rheometer. The sample was investigated using a 25 mm cone-and-plate geometry and heated in a stream of nitrogen. The elastic modulus was measured as a function of temperature with heating and cooling at rates of 1.55 and 1.4 °C/min, respectively, while the sample was being subjected to measurements at the angular frequency $\omega = 10$ rad/s and the strain amplitude $\gamma = 5\%$. Bulk viscosity measurements were conducted using the same geometry with shear rates of $5-100\ s^{-1}$.

C. Small-Angle Neutron Scattering. Small-angle neutron-scattering experiments were performed using the Risø-SANS facility. The bulk copolymer was mounted in a holder with a 1 mm flight path and 1 mm thick Suprasil quartz windows. The aqueous block copolymer solutions were mounted in sealed quartz containers (Suprasil from Hellma, FRG), with 2 mm flight paths.

The results presented below were obtained using the combination of two or more of the scattering patterns obtained with different instrumental settings, using 3, 6, and 14 Å wavelength neutrons, and using a sample-to-detector distance of 1, 3, and 6 m, respectively, giving scattering vectors within the range $0.002-0.5\ Å^{-1}$, where the scattering vector $\bar{q}$ is given by the scattering angle θ and the neutron wavelength λ:

$$|\bar{q}| = q = 4\pi/\lambda \sin(\theta/2) \tag{1}$$

The neutron wavelength resolution was $\Delta\lambda/\lambda = 0.18$, and the neutron beam collimation was determined by the pinhole sizes of 16 and 7 mm diameter at the source and sample positions, respectively, and with the collimation length equal to the sample-to-detector distance. The smearing induced by the wavelength spread, the collimation, and the detector resolution was included in the data analysis discussed below, using Gaussian approximations for the different terms.

The scattering data were corrected for the background arising from the quartz cell D_2O and from other sources, as measured with the neutron beam blocked by plastic containing boron at the sample position. The incoherent scattering from H_2O was used to determine deviations from a uniform detector response and to convert the data into absolute units.

The scattering patterns discussed in the present paper are all azimuthally isotropic. The data have been reduced by azimuthally averaging to the one-dimensional $I(q)$ scattering functions, which are only dependent on the absolute value of $\bar{q}$.

D. Static Light Scattering. Recent papers dealing with light scattering in PS−PEO block copolymer systems are noted in refs 13 and 14, while a general review of scattering in block copolymer systems is given in ref 15. Static light-scattering measurements were made at different temperatures using a photon-counting apparatus supplied by Hamamatsu to register the polarized scattered signal. The light source was a 35 mW He−Ne laser with $\lambda = 633$ nm. The value of $(dn/dc) = 0.15$ mL/g was determined for the PS−PEO 1-3 diblock copolymer at 25 °C using a differential refractometer at the same wavelength.

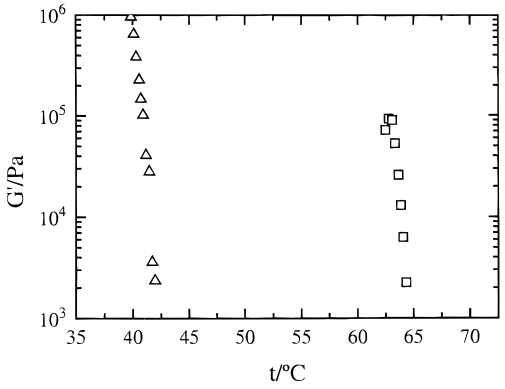

Figure 1. G' measured while heating (□) and cooling (△) the bulk PS−PEO 1-3 sample: cooling rate, 1.55 °C/min; heating rate, 1.4 °C/min; $\omega = 10$ rad/s; $\gamma = 5\%$.

E. Dynamic Light Scattering. Dynamic light scattering, DLS, measurements were made using the apparatus described briefly in ref 16. A wide-band, multi-tau, digital autocorrelator of the 'ALV'-type from Langer GmbH, Germany, was used for data collection. The measured intensity autocorrelation function, $g_2(t)$, is related to the field correlation function, $g_1(t)$, by

$$g_2(t) = B[1 + \beta'|g_1(t)|^2] \tag{2}$$

where β' is an instrumental factor accounting for deviations from ideal correlation and B is a baseline term.

For a continuous distribution of relaxation times, $A(\tau)$, corresponding to an infinite range of particle sizes, the inverse Laplace transform (ILT) may be used:

$$g_1(t) = \int A(\tau) e^{-t/\tau}\, d\tau \tag{3}$$

Such inverse Laplace transformation was performed using a constrained regularization routine, REPES,[17] which minimizes the sum of the squared differences between the experimental and calculated intensity−intensity autocorrelation functions $g_2(t)$ using nonlinear programming and allows the selection of the "smoothing parameter" P (probability to reject). Analysis of data encompassed 288 exponentially-spaced grid points and a grid density of 12 per decade. Representation of the relaxation time distributions in the form of $\tau A(\tau)$ versus $\log(\tau)$ plots, with $\tau A(\tau)$ in arbitrary units, gives an equal area representation.

3. Results and Discussion

A. Bulk Copolymer. *1. Rheology.* The elastic modulus, as measured dynamically in cone-and-plate geometry, is shown in Figure 1. The data are given as a function of temperature for heating and cooling at the rates of 1.55 and 1.4 °C/min, respectively, the measurements being made at the angular frequency $\omega = 10$ rad/s and only a relatively small strain amplitude, $\gamma = 5\%$, in the attempt to avoid changes in the crystalline texture. These mechanical experiments mainly afford transition temperatures. At low temperature, where the material is ordered, the poly(ethylene oxide) block is crystalline while the polystyrene block is glassy. In combination with the low molar mass, this leads to an extremely brittle structure that cannot be reliably mechanically characterized in the cone-and-plate geometry. Any detected signal is mainly due to slippage between the tools and the sample. However, as the temperature is increased, the material

(15) Tuzar, Z.; Kratochvil, P. In *Light Scattering—Principles and Development;* Brown, W., Ed.; Clarendon Press: Oxford, 1996; Chapter 10.

(16) Schillén, K.; Brown, W.; Johnsen, R. M. *Macromolecules* **1994**, *27*, 4825.

(17) Jakes, J. *Czech. J. Phys.* **1988**, *B38*, 1305.

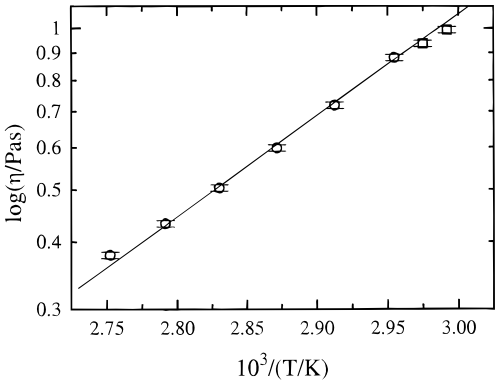

Figure 2. Newtonian viscosity of the bulk PS−PEO 1-3 sample as a function of inverse temperature above T_{ODT} (○) and below T_{ODT} (□). The line is a linear fit to the disordered data.

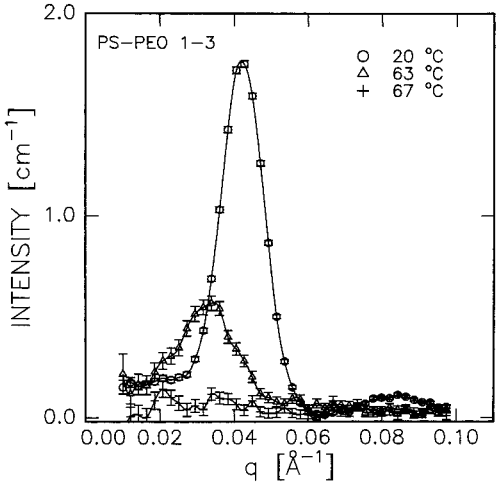

Figure 3. Small-angle neutron-scattering data of bulk PS−PEO 1-3, as obtained at the temperatures 20, 63, and 67 °C.

becomes a paste and a mechanical response can be detected. The modulus drops in a narrow temperature interval (64 ± 1 °C) to a very low level. The sample disorders into a Newtonian liquid with a viscosity close to 1 Pa s. Thus at $\omega = 10$ rad/s, G'' is expected to be 10 Pa s, which is below the sensitivity of the instrument. However, the sharp drop in the modulus can be associated with the disordering process. On cooling, a corresponding sharp rise in modulus is observed at 43 ± 1 °C. This rise in modulus signals the ordering of the sample possibly simultaneously with crystallization of the poly(ethylene oxide) block and glassification of the polystyrene block.

Bulk viscosity results, as measured utilizing shear rates of 5−100 s^{-1}, are given in Figure 2. At all temperatures the sample exhibits Newtonian behavior. The measurements at 63 and 61 °C were conducted after previous heating to 90 °C. The viscosity is nearly proportional to the inverse temperature in the disordered state. A barely significant break in the viscosity is observed on crossing the order−disorder transition temperature, T_{ODT}. However, the ordered state data were obtained after cooling from high temperature, and the sample is disordered according to the dynamical mechanical measurements.

2. Small-Angle Neutron Scattering. Figure 3 shows the scattering function of the PS−PEO 1-3 bulk copolymer as observed at the temperatures $T = 20$ °C, $T = 63$ °C, and $T = 67$ °C. The scattering function clearly reveals a lamellar structure at low temperature, with both first- and second-order peaks. The lamellar periodicity is

$$d = 2\pi/q_{10} = 148 \text{ Å}$$

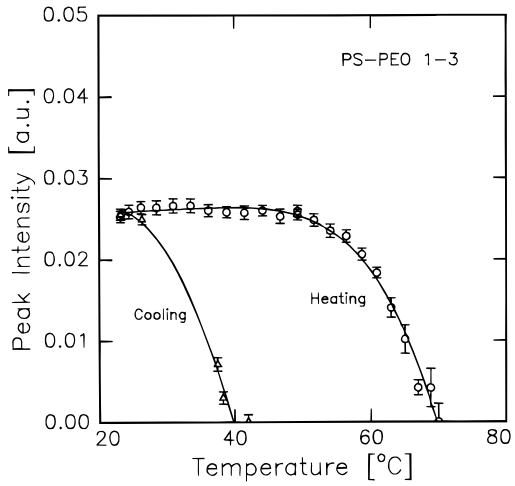

Figure 4. Peak intensity of the lamellar first-order Bragg reflection of PS−PEO 1-3 (Figure 3) as a function of temperature during heating and cooling.

where $q_{10} = 0.0424$ $Å^{-1}$ is the scattering momentum of the first-order Bragg peak. The thickness d_{PS} or d_{PEO} of the respectively PS or PEO lamellae must fulfil

$$d_{PS} = f \cdot d_{10} \quad \text{or} \quad d_{PEO} = (1 - f) \cdot d_{10}$$

where f is the volume fraction of PS. With the mass density 1.05 and 1.01 g/cm^3 of respectively PS or PEO, the molecular configuration of PS−PEO 1-3 gives $f = 0.24$ and thus a PEO lamellae thickness of $d_{PEO} = 112$ Å.

The lamellar structure is most likely a result of crystallization of the PEO blocks, as observed in related PEO systems,[2−6] even though wide-angle scattering has still not been made on PS−PEO 1-3 to verify this.

The observed PEO lamellae thickness $d_{PEO} = 112$ Å is significantly less than the expected value of an unfolded PEO chain with 68 units, irrespective of the helical or zigzag polymorph. In the helical form, the chain length is 2.78 Å per repeat unit (19.48 Å per pitch of 7 units[7]). In the zigzag form, the chain length is 3.56 Å per unit (7.12 per repeat of two units[7]). In the unfolded configuration the PEO block thus should have the length $d_1^{helix} = 195$ Å and $d_1^{zz} = 242$ Å for respectively the helical or zigzag configuration. Related PEO block copolymers have been shown to be in the helical conformation, with the number of chain folds depending on both molecular architecture and crystallization temperature.[8] It is most likely that the PEO block in the PS−PEO 1-3 material behaves similarly. With the values given above, we find that the ratio between the thickness of the PEO lamellae and the length of the unfolded chain is close to 2, thus strongly indicating a single fold in the PEO chain.

Upon heating, the lamellar structure remains basically unaffected up to $T = 50$ °C, where the peak intensity starts to decrease and approaches zero at around $T = 70$ °C, which is slightly higher than the $T_{ODT} = 64$ °C determined from the rheological measurements. These findings indicate that the true ODT is broad and that ordered and disordered domains coexist over a wide temperature interval, in agreement with the strong first-order phase transition. The ODT determined rheologically may reflect the percolation of ordered domains, which would explain the very sharp transition compared to that observed in scattering experiments.

Figure 4 shows the peak intensity as a function of temperature. The values were obtained by fitting a Gaussian function to the experimental data, including instrumental smearing. Simultaneously with the de-

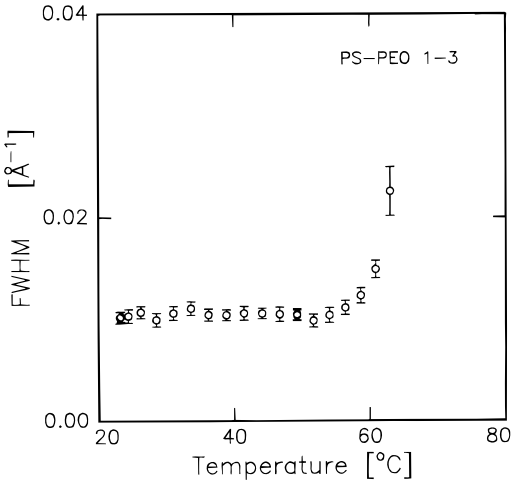

Figure 5. Full width at half maximum of the first-order lamellar Bragg peak of PS−PEO 1-3.

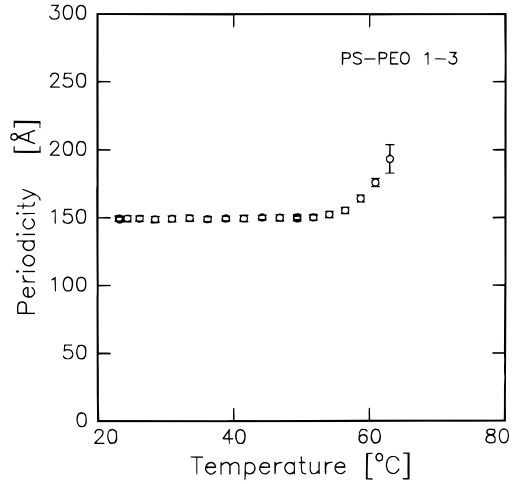

Figure 6. Lamellar periodicity of PS−PEO 1-3 versus temperature.

crease in peak intensity, we observed an increase in peak width, as shown in Figure 5, in agreement with the decreasing size of the ordered domains.

In addition, a pronounced shift to smaller scattering vectors was observed (Figure 6), revealing swelling of the lamellar structure. Close to the highest temperature where the peak can be resolved ($T \sim 70$ °C), the peak position corresponds to a lamellar spacing of 210 Å, corresponding to a PEO thickness of 160 Å. This finding indicates that the PEO chains tend to "unfold" near the order−disorder transition at 70 °C.

In successive cooling stages, we observed a relatively large hysteresis with a 30 °C undercooling before the lamellar structure develops. This is in agreement with the rheological data presented above and expectations for a strong first-order crystallization. The dynamical aspect of this undercooling has, however, not been investigated. The data obtained during heating as well as cooling were obtained stepwise, stabilizing at a given temperature for 10 min and measuring the scattered neutrons within 5 min, corresponding to a mean heating and cooling rate of approximately 0.2 °C/min.

At high temperatures no correlation peak is observable within experimental resolution. This is quite different from observations on the amorphous block copolymers, where there is typically only a relatively small change in peak intensity on crossing the order−disorder transition (ODT). Above the ODT, most block copolymer melts

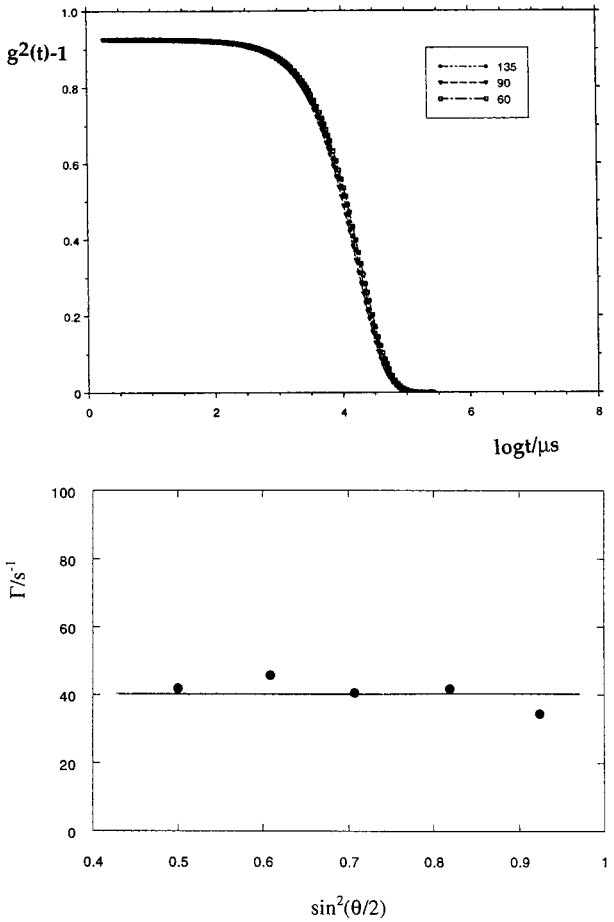

Figure 7. (a, top) Polarized time correlation functions, $g^2(t) - 1$, for the PS−PEO 1-3 melt at three angles and $T = 70$ °C. (b, bottom) Polarized relaxation rate, Γ, as a function of angle for the PS−PEO 1-3 melt at 100 °C.

exhibit a pronounced correlation peak as a result of spatial concentration fluctuations.[18] The peak intensity is, however, given not only by the amplitude of the concentration fluctuations but also by the scattering contrast between the two types of polymer blocks. In the ordered phase of the PS−PEO 1-3 block copolymer, there is only significant contrast between PEO and PS because the PEO block is crystalline whereas PS is amorphous (glass at low T), thus resulting in a marked mass density difference. Above T_{ODT} PEO is also amorphous and the scattering contrast vanishes. Using small-angle neutron scattering, it is therefore not possible to measure any spatial composition fluctuations above the PEO melting temperature, unless the hydrogens in either PS or PEO are substituted with deuterium. Light scattering, as shown below, reveals significant fluctuations in the disordered phase.

3. Light Scattering. Figure 7a shows polarized (VV) correlation functions for the melt copolymer at 67 °C, in close proximity to the order−disorder transition (ODT) at 64 °C and measured at three angles (60, 90, and 135°). Similar measurements were made at 80 and 100 °C. Figure 7b shows the approximately q-independent relaxation rate at 100 °C. Density and reorientational fluctuations are in principle observable in the polarized VV correlation function, while only the reorientational contribution is present in the VH one. Figure 8a demonstrates that the correlation functions are identical in the VV and VH geometries, which indicates strong coupling. We note that

(18) Leibler, L. *Macromolecules* **1980**, *13*, 1602.

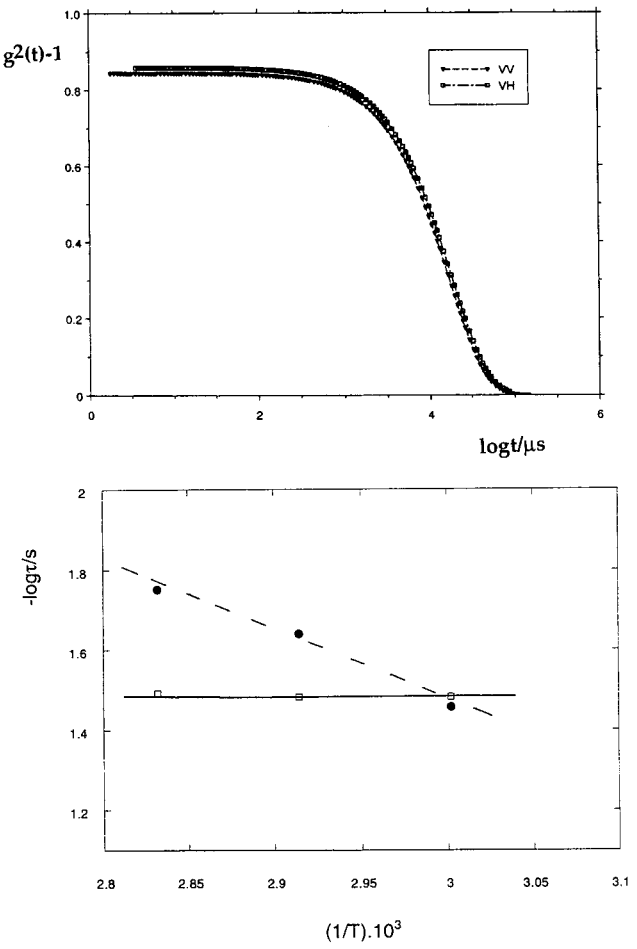

Figure 8. (a, top) Polarized and depolarized correlograms for the melt PS−PEO 1-3 diblock copolymer at 60 °C (order−disorder transition $T_{ODT} \approx 64$ °C). (b, bottom) Arrhenius plots of polarized (□) and depolarized (●) relaxation times for the PS−PEO 1-3 melt.

the VH relaxation time is temperature dependent whereas the VV signal has an insignificant dependence, as is shown in Figure 8b. The slope of the VH line corresponds to an activation energy of 8 kcal/mol. The relative intensities VH:VV are almost constant at about $(I_{VH}/I_{VV}) = 14\%$ over the temperature range 60−100 °C.

The relatively large VV intensities suggest that there are pronounced density fluctuations which are associated with the anisotropy component in the present case. Thus it may be concluded that the single-exponential mode observed in the present experiments is a composite mode reflecting the lamellar domains and their structural anisotropy.

The correlation functions are closely single-exponential with a Williams−Watts (KWW) stretched exponent (β) of approximately unity. The pure single-exponential relaxation essentially eliminates identification of this decay with the segmental motions: the latter would only be observable at the extremely fast limit of the correlator window and are characteristically extremely broad with a KWW exponent in the region 0.2−0.3. It is also unlikely that this relaxation corresponds to the theoretically predicted internal mode, since the latter should also be of short relaxation time and furthermore should not have significant amplitude in the polarized geometry and also should not give rise to depolarized scattering.[19] It should also not be observable for a low MW copolymer.

One possible interpretation for the VH-active component is that it corresponds to the stretching mode. It has been established both experimentally[20,21] and theoretically[22] that in the disordered state close to the ODT the copolymer chains are oriented and stretched. In DLS, such a mode was apparently first observed by Hoffmann et al.,[23] who found that, in diblock melts of polystyrene/polyisoprene close to the ODT, the depolarized spectrum became bimodal: the faster component having $\beta = 0.2$ was due to segmental relaxation, and a slower component having $\beta = 1$ was suggested to be due to orientation and stretching. Jian et al.[24] and Papadakis et al.[25] drew similar conclusions. We note in the present case that the scattered intensity decreases strongly with increasing temperature, which is an expected property of the stretching mode, since the homogeneity of the system increases with increasing temperature. A contribution from the stretching mode in conjunction with reorientation may be expected over an extended temperature range (for a Flory−Huggins parameter above approximately $\chi N \approx 5$[20]) and was observed to be still present far above the fluctuation-induced ODT temperature in a symmetric low molar mass PS−PB diblock copolymer.[25] In the PS−PEO 1-3 diblock copolymer studied here, we should emphasize, however, that the ODT is not driven by composition fluctuations but instead is a result of PEO crystallization into lamellae. Due to the lack of neutron contrast in the disordered phase, we cannot determine the value of the χN parameter.

An alternative explanation in view of the long relaxation time seen in Figure 7a is that advanced by Stepanek et al.[26] The latter suggest that a VH-active mode seen in the low molar mass diblock copolymer melt of poly(ethylenepropylene)−poly(dimethylsiloxane) results from the reorientational dynamics of local regions of lamellar order.

One may use the Stokes−Einstein relationship for the rotational diffusion coefficient ($\Theta = (6/\Gamma)^{-1}$), written in terms of the correlation length ξ_r:

$$\Theta = kT/(8\pi\eta\xi_r^3) \tag{4}$$

where ξ_r will reflect the longest length scale of the anisotropic particle and η is the measured macroscopic viscosity. For the present system, this relationship gives $\xi_r = 460$ Å at 100 °C and 580 Å at 67 °C, just above the ODT. For comparison, the value of the static correlation length, ξ evaluated by fitting the VV intensities measured at different q-vectors to the Ornstein−Zernike equation

$$I(q) \sim I(0)/(1 + \xi^2 q^2) \tag{5}$$

gives a value $\xi = 1120$ Å for the data at 67 °C. The latter is of the same order as ξ_r. The intensities of the VH mode are 8.2 kHz (67 °C) and 5.6 kHz (100 °C); i.e., the amplitude decreases with increasing temperature.

B. Aqueous Solutions. *1. Critical Micelle Concentration*. The value of the cmc = 2.48×10^{-5} g/mL obtained

(19) Stepanek, P.; Lodge, T. P. *Light Scattering—Principles and Development;* Brown, W., Ed.; Clarendon Press: Oxford, 1996; Chapter 11.

(20) Almdal, K.; Rosedale, J. H.; Bates, F. S.; Wignall, G. D.; Fredrickson, G. H. *Phys. Rev. Lett.* **1990**, *65*, 1112.
(21) Bartels, V. T.; Stamm, M.; Abetz, V.; Mortensen, K. *Europhys. Lett.* **1995**, *31*, 81.
(22) Vilgis, T. A.; Weyersberg, A.; Brereton, M. G. *Phys. Rev. E* **1994**, *49*, 3031.
(23) Hoffmann, A.; Koch, T.; Stühn, B. *Macromolecules* **1993**, *26*, 7288.
(24) Jian, T.; Semenov, A. N.; Anastasiadis, S. H.; Fytas, G.; Yeh, F.-J.; Chu, B.; Vogt, S.; Wang, F.; Roovers, J. E. L. *J. Chem. Phys.* **1994**, *100*, 3286.
(25) Papadakis, C. M.; Brown, W.; Johnsen, R. M.; Posselt, D.; Almdal,K. *J. Chem. Phys.* **1996**, *104*, 1611.
(26) Stepanek, P.; Almdal, K.; Lodge, T. P. *J. Polym. Sci., Polym. Phys. Ed.*, submitted.

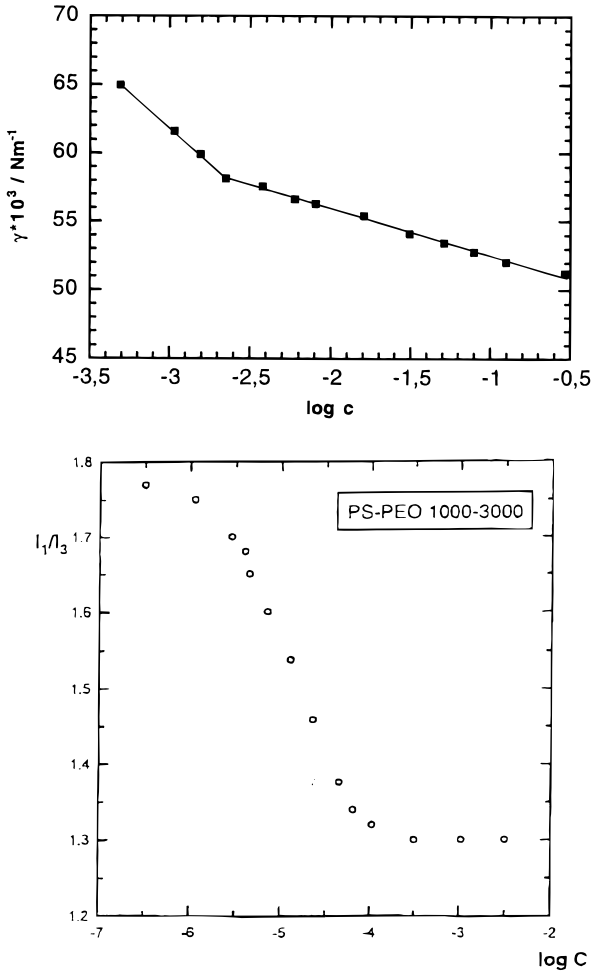

Figure 9. Determination of the critical micelle concentration for the PS−PEO 1-3 diblock copolymer in D_2O at 25 °C using (a, top) surface tension cmc = 2.48 × 10^{-5} g/mL and (b) fluorescence probing with pyrene; cmc = 1.27 × 10^{-5} g/mL.

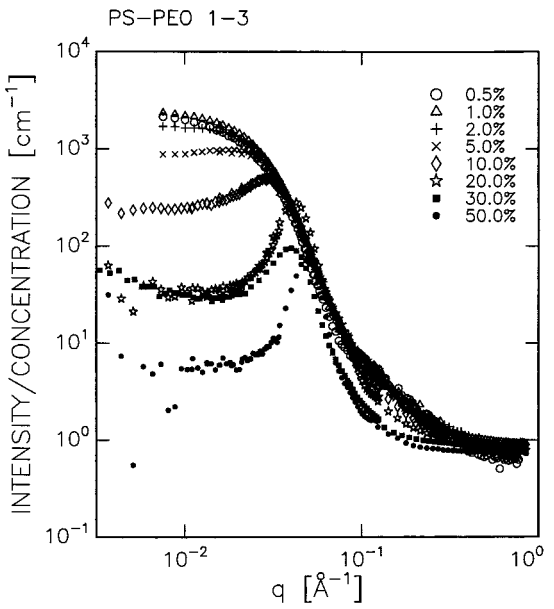

Figure 10. Small-angle neutron-scattering data of aqueous (D_2O) solutions of PS−PEO 1-3, as obtained for concentrations between 0.5% and 50%.

by surface tension measurements (Figure 9a) is somewhat larger than the value reported by Wilhelm et al.[14] ((0.1−0.5) × 10^{-5} g/mL) using a fluorescence method. Using a similar method using pyrene as probe, we obtained the value cmc = 1.27× 10^{-5} g/mL. These data are depicted in Figure 9b.[27]

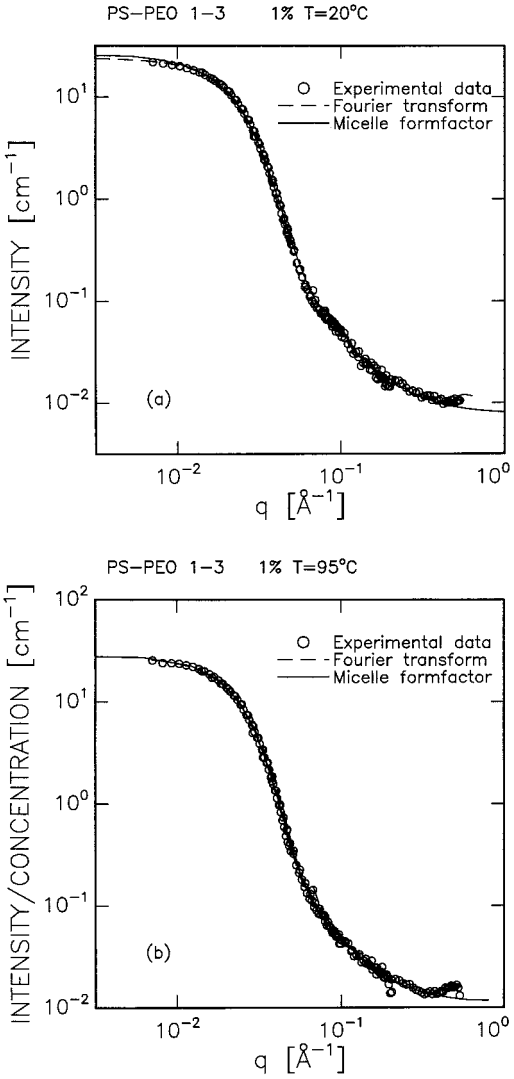

Figure 11. Small-angle neutron-scattering data of 1% aqueous solutions of PS−PEO 1-3, as obtained at (a, top) $T = 20$ °C and (b, bottom) $T = 95$ °C. The solid lines represent the best fit to the micellar form factor. The broken lines represent the fit obtained in the indirect Fourier transformation.

2. Small-Angle Neutron Scattering. In dilute aqueous solutions of PS−PEO 1-3, the scattering function is dominated by the form factor of the copolymer aggregates. For copolymer concentrations of more than a few percent, correlations between the aggregates start to be the dominant feature. Figure 10 shows the scattering function ($I(q)$/concentration) for aqueous solutions of PS−PEO 1-3 diblock copolymer in the concentration regime 0.5−50% in D_2O, as obtained at 20 °C (after being annealed above 60 °C).

The dilute systems (up to roughly 2%) are dominated by the pure form factor of the micelles. For copolymer concentrations up to approximately 20%, the effect of increasing concentration on the scattering function is the development of a correlation hole corresponding to significant intermicellar correlations. For copolymer concentrations above approximately 20%, the scattering function also changes in the high-q regime ($q > 0.05$ Å^{-1}), suggesting changes of the aggregates to a more asymmetric form.

(27) Jada, A.; Hoffstetter, J.; Siffert, B. *Proceedings of Short and Long Chain Interfaces*; Editions Frontiers: 1995; pp 41−46.

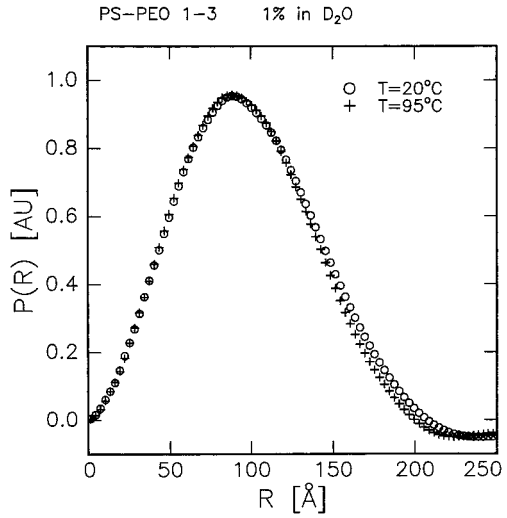

Figure 12. Fourier transform of 1% aqueous solutions of PS−PEO 1-3 as resulting from scattering data obtained at $T = 20$ °C (○) and $T = 95$ °C (+).

Figure 11 shows the scattering function of 1% PS−PEO 1-3 in D_2O as obtained at $T = 20$ °C (after being annealed above 60 °C) and $T = 95$ °C. The structure changes only little over this temperature range.

The $I(q)$-scattering function has been Fourier-transformed using the indirect method of Glatter,[28,29] giving the distance distribution function $p(R)$, which is the scattering density correlation function multiplied by the distance squared. In this method, one uses the form $p(R) = \sum a_n B_n(R)$, where B_n are cubic-spline functions and a_n are parameters to be determined by a constrained least squares analysis. In addition, an independent uniform background describing the incoherent scattering has been included in the data analysis.

Figure 12 shows the resulting distance distribution function $p(R)$, of the 1% PS−PEO 1-3 copolymer concentration, corresponding to the $T = 20$ °C and $T = 95$ °C scattering functions shown in Figure 11. The $p(R)$ function is dominated by a regular bell-shaped form, indicating that the PS−PEO 1-3 copolymers have associated into spherical micellar aggregates, which are relatively monodisperse in size with a radius of the order of 100 Å. The form of the $p(R)$ curve also indicates that intermicellar correlations only have little influence at this low concentration. The radius of gyration, R_g, can be directly calculated from the resulting $p(R)$ function, giving $R_g = 71$ Å and $R_g = 69$ Å at, respectively, 20 and 95 °C.

The scattering function of a spherical block copolymer micelle with a dense core surrounded by a corona of Gaussian polymers can be described analytically, as shown by Pedersen and Gerstenberg[30]

$$F_{mic}(q) = N_{agg}^2 \rho_s^2 F_s(q,R) + N_{agg} \rho_c^2 F_c(q,L,b) + N_{agg}(N_{agg} - 1)\rho_c^2 S_{cc}(q) + 2N_{agg}\rho_s\rho_c S_{sc}(q) \quad (6)$$

where N_{agg} is the aggregation number and ρ_s and ρ_c are the excess scattering length densities of blocks in the core and in the chains, respectively. $F_s(q)$ represents the self-correlation of the spherical core with radius R_c,

$$F_s(q) = \left[\frac{3}{(qR_c)^3}(\sin(qR_c) - qR_c\cos(qR_c))\right]^2 \quad (7)$$

and $F_c(q)$ is the self-correlation of the chains in the corona with radius of gyration R_g

$$F_c(q) \sim x^{-2}(\exp(-x) + x - 1) \quad (8)$$

with $x = (qR_g)^2$. $S_{sc}(q)$ and $S_{cc}(q)$ represents cross-terms which are calculated on the basis of the Debye equation using infinitely thin shells and taking into account the correct weighting functions for, respectively, solid spheres and Gaussian chains. The interference term, $S_{sc}(q)$, between core and chains takes the form[30]

$$S_{sc}(q) = \Phi_s(q,R_c)x^{-1}(1 - e^{-x})\sin(qR_c)/(qR_c) \quad (9)$$

while the interference term between chains attached to the surface, $S_{cc}(q)$, is given by

$$S_{cc}(q) = x^{-2}(1 - e^{-x})^2[\sin(qR_c)/(qR_c)]^2 \quad (10)$$

The solid lines in Figure 11 represent best fits to eq 4, including instrumental smearing and intermicellar correlations, as discussed below. The experimental scattering function is very well represented by this micellar form factor, with effective core sizes $R_c = 56$ Å and $R_c = 53$ Å at respectively 20 and 95 °C. The hard-sphere interaction distance is of the order of 120−140 Å, and the resulting polymer coil of the corona has $R_g = 37$ Å and $R_g = 40$ Å, respectively. While the $p(R)$ function apparently only changes little with increasing temperature, the micellar model fitting to the experimental data indicates some changes in the micellar sizes: reduction in core radius, and thereby reduction in aggregation number, but increase in the degree of swelling of the polymer chains in the corona. The basically unchanged $p(R)$ may be a consequence of these opposing tendencies. The reduction in aggregation number is consistent with the experimental molar mass of the micelles obtained from light scattering, as discussed below.

Higher copolymer concentrations also exhibit only little temperature dependence. The general feature is that, at high temperatures, the low-q scattering increases slightly,

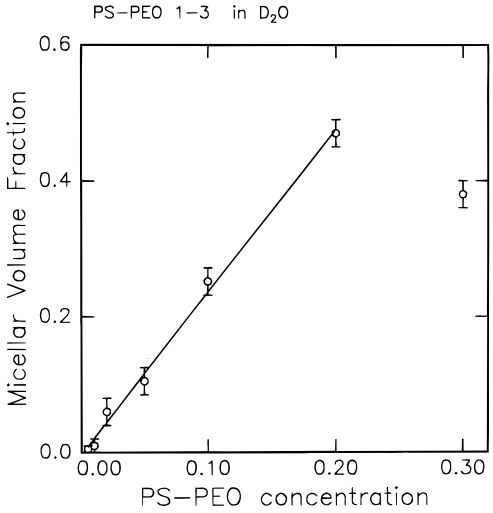

Figure 13. Micellar volume fraction of aqueous solutions of PS−PEO 1-3 from the fit for hard sphere interaction micelles (see text) to the experimental scattering data obtained in the 0.5−30% concentration regime, at $T = 20$ °C.

(28) Glatter, O. *J. Appl. Crystallogr.* **1977**, *10*, 415.
(29) Hansen, S.; Pedersen, J. S. *J. Appl. Crystallogr.* **1991**, *24*, 541.
(30) Pedersen, J. S.; Gerstenberg, M. *Macromolecules* **1996**, *29*, 1363.

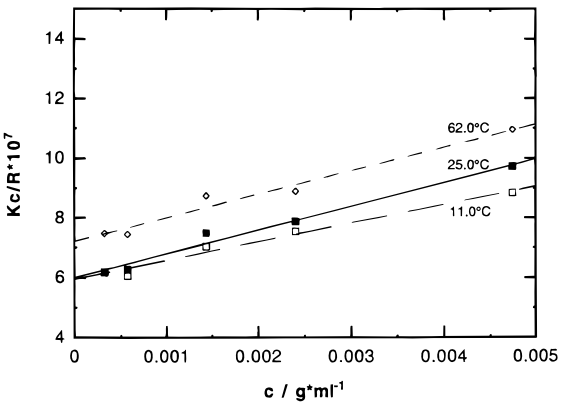

Figure 14. Static light-scattering data on dilute solutions of PS−PEO 1-3 diblock copolymer in D_2O at three temperatures as shown.

whereas the scattering at $q > 0.05$ Å^{-1} remains roughly unchanged.

When the copolymer concentration is increased to between 5 and 10%, the only effect on the scattering function is the formation of a correlation hole due to intermicellar correlations. The scattering function can be well fitted by fixing the micellar parameters at the values for the 1% solution, leaving the micellar volume fraction and interaction radius as the only remaining parameters to be obtained.

Such fits give a linear increase in the micellar volume fraction ϕ with copolymer concentration c in the range 0−20%, effectively corresponding to a critical micellation concentration, cmc ≈ 0, in agreement with the cmc determined from fluorescence and surface tension measurements discussed above, and a slope of $\phi/c = 2.4$ (Figure 13). The linear relationship is self-consistent with the assumption that the micellar form is independent of copolymer concentration. Figure 13 includes fits up to 30%. For these high-concentration suspensions, however, there are some discrepancies between the fitted analytical function and the experimental data, possibly indicating that the micelles are nonspherical for c larger than roughly 20%. Dynamic light scattering, as discussed below, also indicates formation of larger, possibly asymmetric aggregates and shows coexistence of the spherical micelles and larger aggregates for concentrations above 10%.

From the resulting core size, one can estimate the aggregation number of the spherical micelles assuming that the core consists solely of polystyrene:

$$N_{agg} = 4\pi/3 \cdot R_c^3/V_{PS} \quad (11)$$

where $V_{PS} = 1.65 \times 10^3$ Å^3 is the volume of the PS block, giving $N_{agg} = 470$ at ambient temperature. Independently, the aggregation number can be evaluated by combining information on the hard sphere radius and the volume fraction:

$$N_{agg} = c/\phi \cdot 4\pi/3 \cdot R_{hs}^3/V_{PS-PEO} \quad (12)$$

where $V_{PS-PEO} = 6.59 \times 10^3$ Å^3 is the volume of the whole block copolymer, giving $N_{agg} = 460$, in very good agreement with the calculation from the core size.

3. Static Light Scattering. The molar mass of the micelles in dilute solution ($C < 0.3\%$) was determined by static light scattering as a function of temperature in the range 10−70 °C. Typical data are shown in Figure 14 at three temperatures: 11, 25, and 62 °C. The value $M = 1.7 \times 10^6$ at 11 and 25 °C corresponds to an aggregation number of 425. The molar mass is lower (1.4×10^6) at the higher temperature of 62 °C, in good agreement with the observed 5% reduction in core radius R_c discussed above. Since the cmc is extremely low (as indicated from the results of Figures 9 and 13 above), the concentrations used in static light scattering have not been corrected for the cmc.

The micelles are sufficiently small that there is no detectable angular dependence of the reduced intensity over the range $\theta = 20-140°$. An estimate of the micellar radius can, however, be made from the second virial coefficient ($A_2 = 6.2 \times 10^{-5}$ mL mol g^{-2} at 25 °C) using the

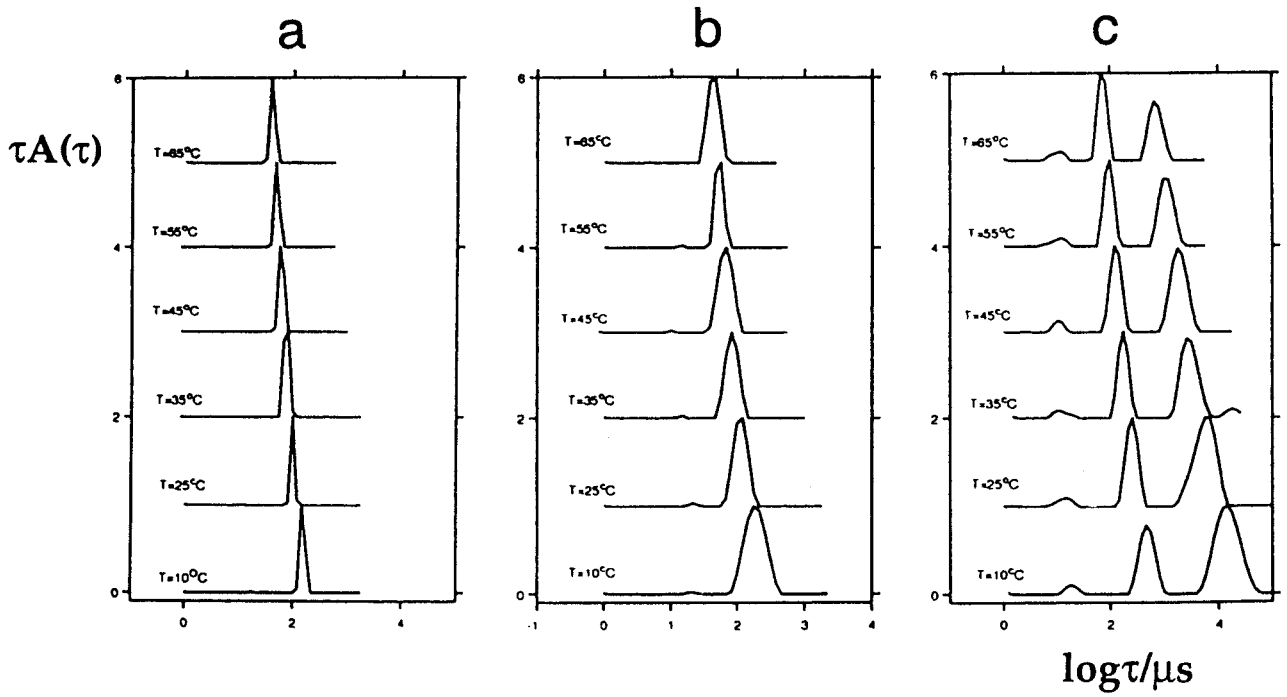

Figure 15. Inverse Laplace transform relaxation time distributions from dynamic light scattering at (a) 2.3%, (b) 5%, and (c) 20% PS−PEO 1-3 in D_2O at different temperatures as indicated. Measurements at an angle of 90°.

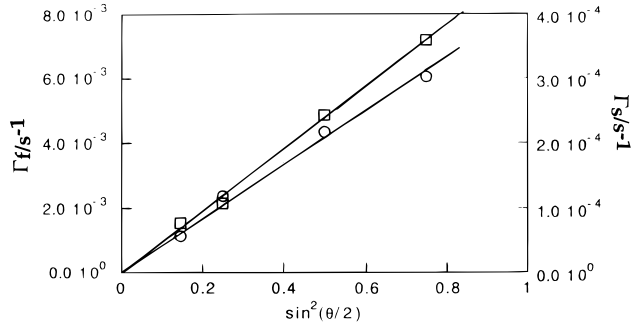

Figure 16. Dependence of the relaxation rate (Γ) on $\sin^2(\theta/2)$ for the fast (left axis, □) and slow (right axis, ○) modes at c = 20% in D_2O and 25 °C.

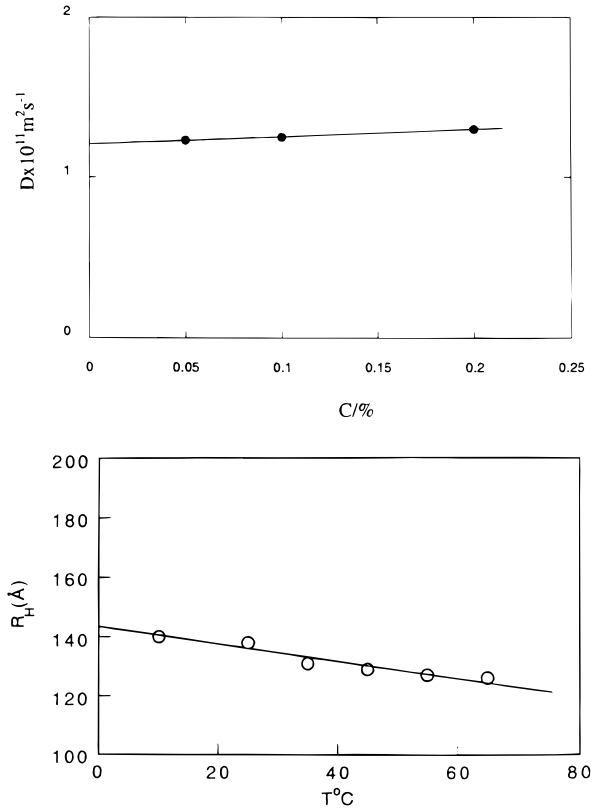

Figure 17. (a, top) Dependence of the dilute solution diffusion coefficient, D, on PS−PEO 1-3 concentration in D_2O, at T = 25 °C. (b, bottom) Dependence of the PS−PEO 1-3 hydrodynamic radius, R_h (from the infinite dilution values of the diffusion coefficient), as a function of temperature.

relationship[31]

$$R_{A_2} = [3M^2A_2/(16\pi N_A)]^{1/3} \qquad (13)$$

The obtained value, R_{A_2} = 170 Å, corresponds to the effective radius of interaction and should coincide with the hard sphere radius, R_{hs} = 120−140 Å. The R_{A_2} value is also somewhat *larger* than the hydrodynamic radius (R_h = 140 Å) derived from the translational diffusion coefficient extrapolated to infinite dilution—see below. Alternatively, one may estimate the dimensions from the intrinsic viscosity [η] using the relationship for the volume, V_h, of a spherical particle:

$$V_h = M[\eta]/2.5N_A \quad \text{and} \quad V_h = (4/3)\pi R_h^3 \qquad (14)$$

(31) Yamakawa, H. *Modern theory of polymers solutions*; Harper & Row: New York, 1971.

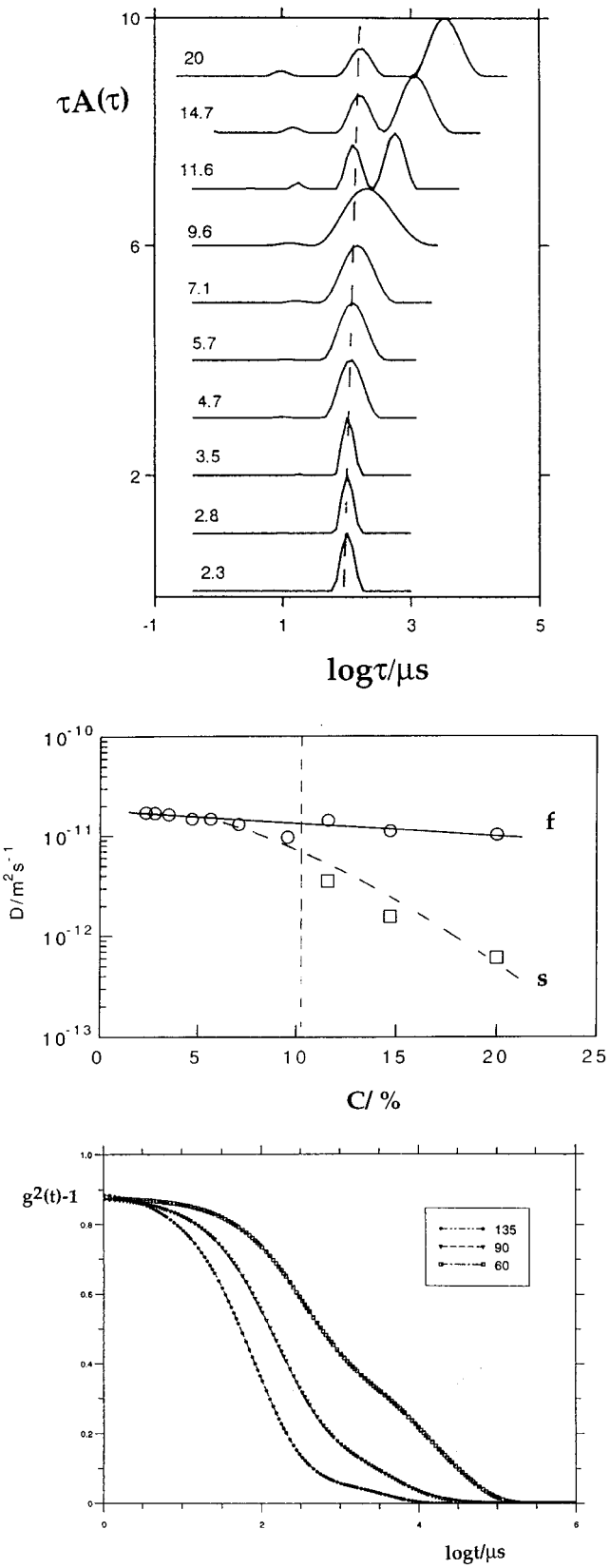

Figure 18. (a, top) Relaxation time distributions at different concentrations (in %) of PS−PEO 1-3 in D_2O at 25 °C. (b, center) Log−lin plot of diffusion coefficients for PS−PEO 1-3 diblock copolymer in D_2O at 25 °C, corresponding to the distributions in Figure 17a. (c, bottom) Time correlation functions (polarized) at three angles as shown. Data for C = 10% and 25 °C.

Using the measured value of the intrinsic viscosity [η] = 12.9 mL/g leads to R_h = 120 Å.

These values are of the same magnitude as those reported by Xu et al.[13] (R_h = 200 Å) using DLS and are

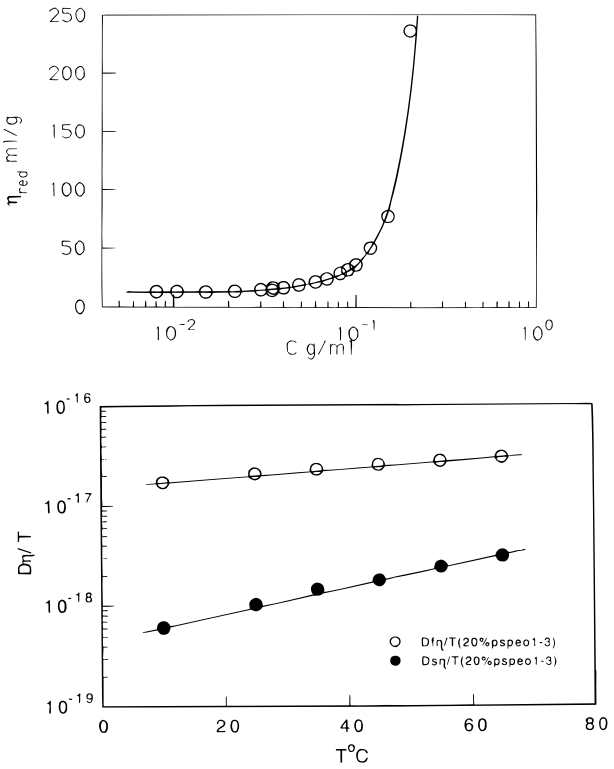

Figure 19. (a, top) Concentration dependence of reduced viscosity (T = 25 °C) for PS−PEO 1-3 diblock copolymer in D_2O. (b, bottom) Temperature dependence of the reduced diffusion coefficient for the fast (upper) and slow (lower) modes at C = 20%.

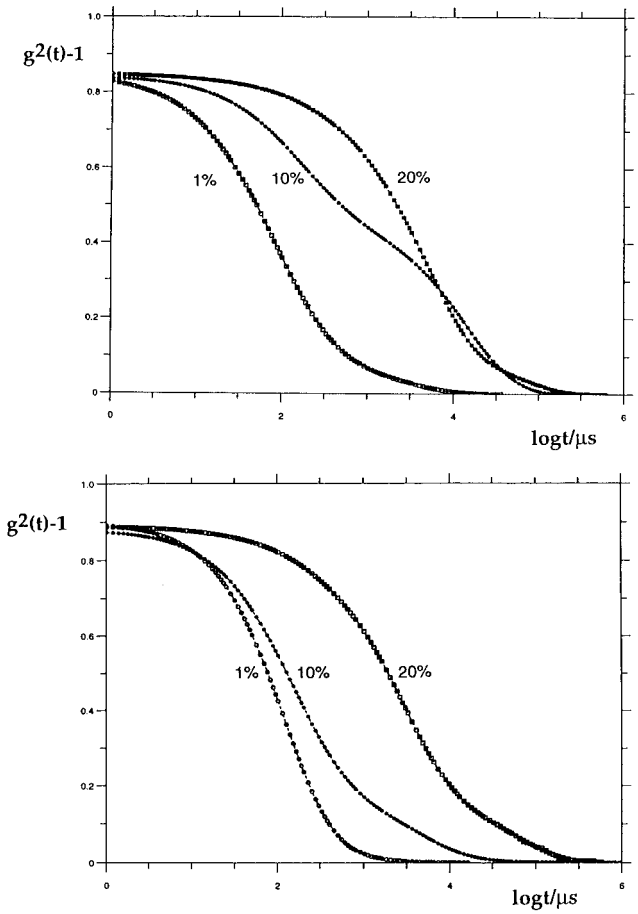

Figure 20. (a, top) Depolarized (VH) time correlation functions at three concentrations as shown for PS−PEO 1-3 diblock copolymer at T = 25 °C. (b, bottom) Corresponding polarized (VV) correlograms corresponding to part a.

also in good agreement with the SANS data described above.

4. Dynamic Light Scattering. In dynamic light-scattering studies, the autocorrelation functions in the dilute range (c < 5%) were close to single exponential. Examples of the relaxation time distributions obtained using the Laplace inversion routine REPES (see Experimental Section) are given at three concentrations [(a) 2.3%; (b) 5%; (c) 20%] for different temperatures in Figure 15. The dependence of the relaxation rate on the square of the scattering vector (q) was linear (Figure 16) for both modes in part c, passing through the origin, denoting diffusive processes. The concentration dependence of the diffusion coefficient is small; see Figure 17a. Use of the Stokes−Einstein equation ($R_h = kT/6\pi\eta_0 D_0$) together with the infinite dilution value, D_0, and the solvent viscosity, η_0, gave R_h = 140 Å at 25 °C. The temperature dependence of R_h is shown in Figure 17b.

With increasing concentration the relaxation time distribution broadens and eventually becomes double exponential above about c = 10% as shown in Figure 18a and b. Polarized correlation functions are shown for c = 10% at three angles in Figure 18c.

The inverse intrinsic viscosity corresponds to an approximate value of the "overlap" concentration of c^* = 8%. The concentration dependence of the slow mode is much stronger and may correspond to the development of micellar clusters above the overlap concentration. On the basis of the neutron scattering data discussed above, however, it seems more likely that differently shaped micelles are formed, possibly in the form of wormlike aggregates with significant anisotropy (see below). The present structural data cannot, however, give unambiguous detail on the structure of these large aggregates. Figure 19a shows how the reduced viscosity η_{red} varies as a function of concentration. There is a slow increase above c^* and then a strong increase above about 10%. Figure 19b shows the temperature dependence of the reduced diffusion coefficient for fast and slow modes at c = 20%.

The appearance of the slow mode at about 10% is seen clearly in Figure 20a, which shows the depolarized correlation functions. The correlation function at c = 10% is bimodal whereas that for c = 20% is dominated by the slower relaxing process.

A comparison with the corresponding polarized correlation functions is provided by Figure 20b for the three concentrations. The enhanced depolarized scattering for the slower part reflects a small but significant anisotropy associated with the slow mode (I_{VH}/I_{VV}) = 2%. At c = 20% the VV and VH correlation functions are again very similar, due to strong coupling between the relaxational modes.

The appearance of the slow mode most likely reflects residual aggregation into larger, wormlike micelles. Large aggregates have correspondingly been noted in the light-scattering study of Winnik et al.[13] The driving force is the interaction between the PS blocks and water, which promotes segregation of the PS blocks. From the slow mode diffusion coefficients (D(25 °C = 5.3 × 10^{-14} m^2 s^{-1} (20%) and 2.9 × 10^{-13} m^2 s^{-1} (10%)) and the determined macroscopic viscosities (η(25 °C = 42.9 × 10^{-3} Pa s (20%) and 7.75 × 10^{-3} Pa s (10%)), R_h for the slow mode equals 970 Å at both 10% and 20%. From the strong concentration dependence of the slow relaxation, it is thus concluded that the number density of the aggregates increases but their size does not change significantly with concentration.

Assuming a rodlike structure, one can estimate the rod length from the expression[32]

$$R_h = L/[2\sigma - 0.19 - (8.24/\sigma) + (12/\sigma^2)] \quad (15)$$

where $\sigma = \ln(L/r)$ with r being half the rod thickness. Using the value $r = 140$ Å (i.e. the radius of the spherical micelles at low concentrations) and with $R_h = 970$ Å, the value $L = 5500$ Å is obtained.

4. Summary

PS−PEO 1-3 in the bulk forms a low-temperature lamellar ordered phase induced by the PEO crystallization into sheets. In the temperature range 50−70 °C a broad transition into a disordered phase is observed. The disordered phase is characterized by major concentration fluctuations, as revealed by the DLS data and which may reflect the dynamics of incipient lamellar regions as the ODT is approached. The order−disorder transition thus has a large hysteresis, as expected when the order is induced as a result of PEO crystallizing into lamellae directly from the disordered phase. The dynamical aspect of this hysteresis (or undercooling) remains, however, to be studied.

In aqueous solutions, PS−PEO 1-3 over wide concentration ranges (up to roughly 20% polymer concentration) forms spherical micelles of aggregation number of the order of 420−470. The micelles are very temperature stable. On raising the temperature from ambient to 95 °C, the spherical aggregates change only slightly, giving rise to an approximately 5% reduction in core size and a corresponding ~15% reduction in aggregation number but a somewhat swollen corona.

Above $c = 10\%$, a slow relaxation process is evident, which is associated with a strong increase in the solution viscosity. Since this feature is also anisotropic, it is suggested that it reflects the formation of large wormlike aggregates.

Acknowledgment. This work has been supported by the Swedish Research Council (NFR) and the Danish Polymer Centre sponsored by the Program for Development of Materials Technology. We are grateful to Ida Lidegran for assistance with the light-scattering measurements and Göran Svensk, Uppsala, for the surface tension and viscosity measurements. We would like to thank A. Ryan for helpful discussions and access to a preprint of ref 8.

LA9609635

(32) Young, C. Y.; Missel, P. J.; Mazer, N. A.; Benedek, G. B. *J. Phys. Chem.* **1978**, *82*, 1375.